Journal of Engineering Science 16(1), 2025, 93-102
DOI: https://doi.org/10.3329/jes.v16i1.82670

JES
an international Journal

SOLVENT FREE MECHANO-CHEMICAL APPROACH FOR THE PREPARATION OF MANGANESE DIOXIDE AS CATHODE COMPONENT FOR AQUEOUS RECHARGEABLE ZINC ION BATTERIES

Parbhej Ahamed[1*], Zahid Hasan[1], Nusrat Tazeen Tonu[1, 2], Md. Abdus Salam[3] and Mohammad Abu Yousuf [1]

[1]*Department of Chemistry, Khulna University of Engineering & Technology (KUET), Khulna-9203*
[2]*Chemistry Discipline, Khulna University, Khulna 9208, Bangladesh*
[3]*Department of Chemistry, University of Dhaka, Dhaka-1000, Bangladesh*

Received: 07 March 2025 Accepted: 21 June 2025

ABSTRACT

Aqueous rechargeable zinc-ion batteries (ARZIBs) have emerged as promising candidates for cost-effective and environmentally friendly energy storage solutions. However, achieving energy densities comparable to commercial lithium-ion batteries requires the development of advanced cathode materials. In this study, we present a simple, solvent-free mechano-chemical method for synthesizing manganese dioxide (MnO_2) as a cathode material for ARZIBs. The structural and morphological properties of the prepared MnO_2 were characterized using Fourier Transform Infrared Spectroscopy (FTIR), X-ray Diffraction (XRD), Energy-Dispersive X-ray Spectroscopy (EDX) and Scanning Electron Microscopy (SEM). The FTIR spectrum showed a characteristic Mn–O stretching vibration at 529 cm^{-1}, while XRD confirmed the formation of a tetragonal α-MnO_2 phase. SEM analysis revealed porous surface morphology with particle size variation, and EDX confirmed the elemental composition of Mn and O only. Electrochemical performance was evaluated using cyclic voltammetry (CV) at a scan rate of 1 mV/s in a CR2032 coin cell, which exhibited distinct and reversible redox peaks. These results indicate the effectiveness of the prepared MnO_2 as a viable cathode material for aqueous zinc-ion batteries.

Keywords: *MnO_2 material, Mechano-chemical method, Aqueous Rechargeable Batteries.*

1. INTRODUCTION

The global industrial and technological revolution of the 21st century has been largely driven by an ever-increasing demand for energy. From consumer electronics and transportation systems to large-scale industrial applications and smart grids, energy storage systems have become an indispensable component of modern infrastructure. The escalating consumption of electricity, largely fueled by the growing global population and increasing urbanization, has made it imperative to develop reliable, efficient, and sustainable energy storage technologies. Traditional energy sources such as fossil fuels have historically met the world's energy demands. However, their widespread use has resulted in numerous environmental challenges, including greenhouse gas emissions, global warming, and environmental degradation. In response, there is a paradigm shift toward clean and renewable energy sources such as solar, wind, hydro, and tidal energy (Idota *et al*., 1997; Chauhan *et al*., 2014; Xiang *et al*., 2012; Marepalli *et al*., 2020). These sources are environmentally friendly and theoretically limitless. However, their intermittent and variable nature poses significant challenges for energy reliability and availability, as they are often dependent on location, time of day, and weather conditions.

To address these limitations, the role of high-performance energy storage systems has become more crucial than ever. Efficient energy storage solutions can bridge the gap between energy generation and consumption, storing surplus energy during peak production times and releasing it during periods of high demand or low generation. This functionality is essential to the successful integration of renewable energy into the global energy mix. The concept of storing electrical energy dates back centuries. The foundation of battery technology was laid by William Gilbert in the 1600s and later advanced by Alessandro Volta, who created the first true battery in the early 1800s. Since then, battery technology has seen a remarkable evolution in both materials and configurations. Early batteries such as lead-acid and nickel-cadmium offered rudimentary performance but laid the groundwork for modern electrochemical storage devices.

In recent decades, lithium-ion batteries (LIBs) have revolutionized the energy storage landscape due to their high energy density, light weight, and long cycle life (Huang *et al*., 2019; Arshad *et al*., 2020). LIBs have

---

*Corresponding Author: *parbhej@chem.kuet.ac.bd* become the backbone of portable electronics, electric vehicles, and grid storage solutions. However, despite their widespread adoption, LIBs are not without limitations. The use of flammable organic electrolytes presents safety risks such as leakage, fire, and explosion under extreme conditions. Moreover, lithium is a relatively scarce and geographically concentrated resource, making LIBs expensive and geopolitically sensitive. Environmental concerns related to lithium extraction, processing, and disposal further complicate their sustainability (Dehghani-Sanij *et al*., 2019; Serra *et al*., 2022; Xu *et al*., 2008; Goodenough *et al*., 2010). The drawbacks of LIBs particularly related to cost, safety, and resource limitations have spurred global efforts to identify alternative battery chemistries that are safer, more sustainable, and economically viable. Among the various emerging battery technologies, aqueous rechargeable zinc-ion batteries (ARZIBs) have gained significant attention in recent years. Zinc, unlike lithium, is abundantly available in the Earth's crust, inexpensive, and non-toxic. Its use in aqueous systems further enhances the safety profile of ARZIBs, as water-based electrolytes are non-flammable, environmentally benign, and cheaper than organic solvents used in LIBs (Blanc *et al*., 2020; Hu *et al*., 2019; Hilder *et al*., 2012).

ARZIBs operate using a zinc metal anode, an aqueous electrolyte (typically zinc sulfate or zinc acetate), and a suitable cathode material capable of reversible Zn^{2+} ion intercalation and deintercalation. Zinc metal itself offers a high theoretical specific capacity of 820 mAh g^{-1} and a relatively low redox potential (-0.76 V vs. SHE), making it an attractive anode material. Additionally, zinc's ability to be safely handled, transported, and stored under ambient conditions gives it a logistical advantage over lithium. These characteristics make ARZIBs highly suitable for large-scale energy storage applications, especially in stationary storage systems for renewable energy and backup power. Their low cost and enhanced safety also make them appealing for off-grid and rural electrification in developing regions. Despite the advantages of ARZIBs, the choice of cathode material remains a critical determinant of their electrochemical performance. A suitable cathode must accommodate the reversible insertion and extraction of Zn^{2+} ions while maintaining structural stability, high capacity, good electronic conductivity, and long cycle life. Numerous cathode materials have been explored for ARZIBs, including: manganese-based oxides (Zhang *et al*., 2022; Tonu *et al*., 2024), vanadium-based oxides (Liao *et al*., 2020), Prussian blue analogs (PBAs) (Nie *et al*., 2014), organic compounds and polymers (Meng *et al*., 2022), and polyanionic materials.

Each class has its advantages and limitations. For instance, vanadium-based materials have shown promising capacities exceeding 300 mAh g^{-1} and excellent cyclability. However, their high cost, environmental toxicity, and narrow operational voltage windows (~1.0 V vs. Zn/Zn^{2+}) reduce their practicality for commercial deployment (Li *et al*., 2020; Lu *et al*., 2017; Zhang *et al*., 2015; Tian *et al*., 2020). Similarly, Prussian blue analogues exhibit a high operating voltage (1.5–1.7 V vs. Zn/Zn^{2+}), but their limited specific capacity (50–120 mAh g^{-1}) restricts their utility in high-energy applications (Ma *et al*., 2019; Deng *et al*., 2014). Among the various materials investigated, manganese-based oxides have emerged as front-runners due to their abundance, affordability, low toxicity, and favorable electrochemical properties. They exhibit a broad range of oxidation states, allowing various structural configurations and redox mechanisms to be employed in Zn^{2+} intercalation processes (Yang *et al*., 2019; Zhou e*t al*., 2021; Chamoun *et al*., 2018). Manganese dioxide (MnO_2) is one of the most widely studied manganese oxides for battery applications. It exists in several polymorphic forms, including α-, β-, γ-, and δ-MnO_2, each with different tunnel or layered structures conducive to Zn^{2+} ion diffusion. Among these, α-MnO_2 is of particular interest due to its large (2 × 2) tunnel structure that can accommodate hydrated zinc ions with minimal structural distortion (Li *et al*., 2021; Xu *et al*., 2012; Xu *et al*., 2012).

MnO_2 has a high theoretical capacity of approximately 308 mAh g^{-1} and operates within a suitable voltage range of 1.3–1.35 V vs. Zn/Zn^{2+}. Its wide natural availability and environmental compatibility make it an ideal candidate for sustainable battery design. However, several challenges hinder its practical application. Bulk MnO_2 exhibits: poor intrinsic electrical conductivity, pronounced volume changes during Zn^{2+} intercalation/deintercalation, structural degradation over long-term cycling, phase transformations that reduce reversibility and efficiency (Jiao *et al*., 2007).

In order to address the aforementioned limitations, researchers have developed various strategies to improve the electrochemical performance of MnO_2, including nano-structuring, composite formation, and doping with conductive additives. A critical aspect of improving cathode materials lies in the choice of synthesis method, which directly influences the morphology, crystallinity, surface area, and defect density of the final product. A variety of synthesis techniques have been employed to tailor the physicochemical properties of MnO_2. These include hydrothermal synthesis (Hashemzadeh *et al*., 2009), micro-emulsion method (Guan *et al*., 2018; Tonu *et al*., 2025), molten salt synthesis **(**Huang *et al*., 2021), solvothermal synthesis **(**Zhang *et al*., 2020), solid-state and combustion methods (Tonu *et al*., 2024**).** While these techniques can produce high-performance MnO_2, they often suffer from drawbacks such as high energy consumption, long processing times, low scalability, and environmental concerns due to the use of solvents or toxic precursors.

In recent years, solvent-free mechano-chemical synthesis has gained attention as a green, efficient, and scalable method for preparing advanced materials. This technique involves the use of mechanical energy (typically through ball milling or grinding) to induce chemical reactions between solid precursors at ambient temperature, eliminating the need for solvents or high-temperature treatment. This study proposes a solvent-free mechano-chemical synthesis approach as a promising strategy to produce MnO_2 with enhanced structural and electrochemical characteristics, aligned with the goals of green chemistry and industrial scalability. The findings from this research are expected to contribute to the development of next-generation, sustainable energy storage systems.

2. MATERIALS AND METHODS

2.1 Materials

All chemicals used in this study were of analytical grade and obtained from reputable commercial suppliers. They were used as received, without any further purification. Detailed information regarding the materials employed in the experimental procedures is presented in Table 1.

Table 1. Lists of the used materials

Materials	Sources
Potassium permanganate ($KMnO_4$)	Loba Chemie, India
Potassium iodide (KI)	Loba Chemie, India
Carbon Black (C)	Fine carbon, China
Polyvinylidene (PVDF)	Loba Chemie, India
N-methyl pyrolidone (NMP)	Sigma Aldrich, USA
Zinc Sulphate ($ZnSO_4$)	Merck, India
Filter Paper	Whatman, GE Healthcare UK
Zinc Foil	TOB, China
Stainless steel foil	TOB, China
Acetone (CH_3COCH_3)	Merck, India
Distilled water	Department of Chemistry, KUET

2.2 Synthesis of MnO_2 Material

A stoichiometric mixture of analytical-grade potassium permanganate ($KMnO_4$) and potassium iodide (KI) was manually ground in an agate mortar using a pestle for 30 minutes to ensure homogeneity. The resulting powder was then transferred to a crucible and subjected to thermal treatment in a muffle furnace at 500 °C for 3 hours to facilitate the formation of manganese dioxide (MnO_2). Following calcination, the synthesized MnO_2 was thoroughly washed multiple times with Millipore-grade deionized water using a Büchner funnel to remove residual impurities and by-products. The washed material was then placed in a clean crucible and dried in a laboratory oven at 105 °C for 6 hours. The resulting MnO_2 powder was stored in sealed glass vials at room temperature for further use. Comprehensive material characterization was performed using Fourier Transform Infrared Spectroscopy (FTIR), X-ray Diffraction (XRD), Energy Dispersive X-ray Spectroscopy (EDS), and Scanning Electron Microscopy (SEM).

2.3 Fabrication of CR2032 Coin Cell

CR2032-type coin cells were assembled using the synthesized MnO_2 as the cathode active material. A homogeneous slurry was prepared by mixing MnO_2 powder, conductive carbon black (C), and polyvinylidene fluoride (PVDF) binder in a weight ratio of 7:2:1, respectively, using N-methyl-2-pyrrolidone (NMP) as the solvent. The resulting slurry was uniformly coated onto a stainless steel foil current collector and subsequently dried in a vacuum oven to remove residual solvent. A 2 M zinc sulfate ($ZnSO_4$) aqueous solution was employed as the electrolyte. Whatman filter paper was used as the separator, and a zinc foil served as the anode. The components were assembled into a CR2032 coin cell configuration under ambient conditions for subsequent electrochemical testing.

3. RESULTS AND DISCUSSION

Figure 1 presents a schematic illustration of the manganese dioxide (MnO_2) synthesis process using a solvent-free mechano-chemical approach.

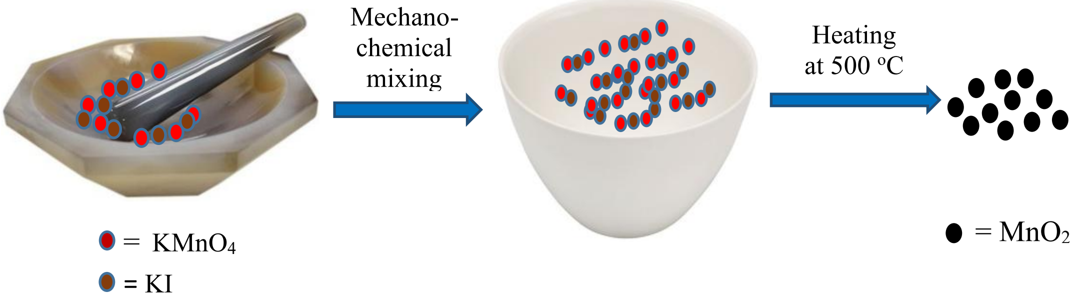

Figure 1: Schematic illustration of the preparation of MnO_2 materials.

In the initial step, stoichiometric amounts of potassium permanganate ($KMnO_4$) and potassium iodide (KI) were introduced into an agate mortar. The reactants were thoroughly ground using a pestle to ensure uniform mixing and initiate the solid-state reaction. The resulting powder was subsequently transferred into a crucible and subjected to thermal treatment in a muffle furnace at 500 °C. The formation of MnO_2 occurred according to the following chemical reaction:

$$KMnO_4\ (s) + KI\ (s) = MnO_2\ (s) + I_2\ (g) + K_2O\ (s)$$

3.1 FTIR Analysis

Fourier Transform Infrared Spectroscopy (FTIR) was employed to investigate the vibrational characteristics and confirm the presence of Mn–O bonds in the synthesized MnO_2 material. The FTIR spectrum, recorded over the wavenumber range of 400–4000 cm^{-1}, is presented in **Figure 2**.

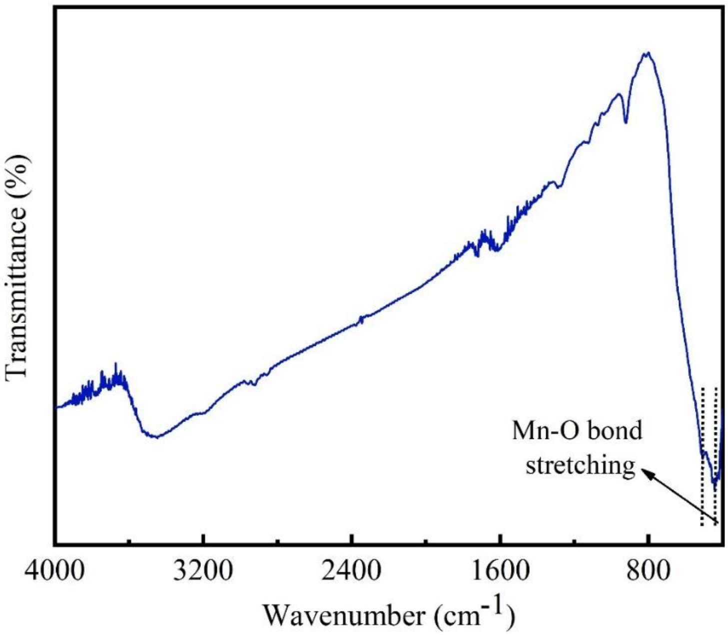

Figure 2: FTIR spectrum of the prepared MnO_2 material.

Prominent absorption bands were observed at approximately 3416 cm^{-1} and 1614 cm^{-1}, corresponding to the O–H stretching and bending vibrations, respectively. These signals are attributed to surface-adsorbed water molecules on the MnO_2 material (Hu *et al.*, 2011; Tang *et al.*, 2010; Wang *et al.*, 2007). A distinct peak at around 507 cm^{-1}, along with a weaker band near 463 cm^{-1}, is indicative of Mn–O stretching vibrations within the MnO_2 crystal lattice (Wang *et al.*, 2008; Mim *et al.*, 2023). Additionally, the absorption band at approximately 1030 cm^{-1} is associated with Mn–OH bending vibrations, suggesting interactions between hydroxyl groups and manganese atoms (Parida *et al.*, 2009; Ahamed *et al.*, 2023). These spectral features confirm the successful formation of MnO_2 and provide insights into the chemical bonding and surface characteristics of the synthesized material.

3.2 XRD Analysis

Powder X-ray Diffraction (XRD) analysis was conducted to investigate the crystalline structure and phase purity of the synthesized MnO_2 material. The XRD pattern of MnO_2, prepared via the solvent-free mechanochemical method and thermally treated at 500 °C, is presented in **Figure 3**.

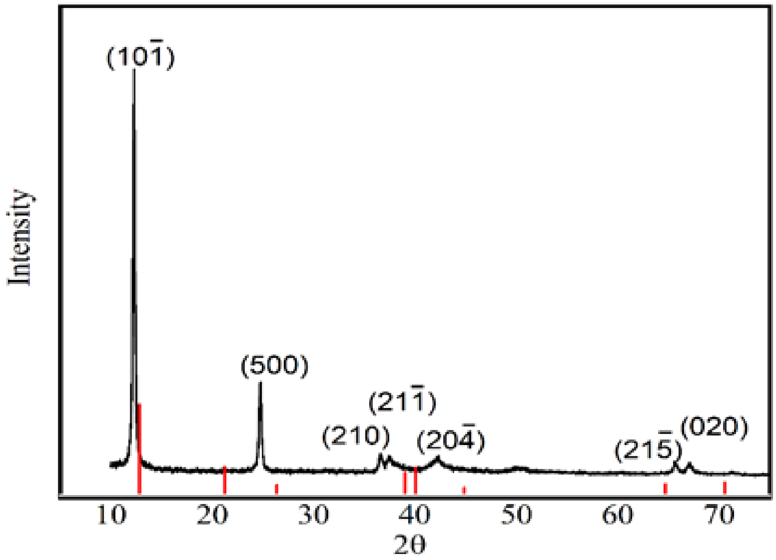

Figure 3: XRD patterns of the prepared MnO_2.

The diffraction pattern confirms the crystalline nature of the MnO_2 sample. Distinct peaks observed in the diffractogram correspond to the $(10\bar{1})$, (500), (210), $(21\bar{1})$, $(20\bar{4})$, $(21\bar{5})$, and (020) crystal planes. These reflections are in good agreement with standard reference data for the tetragonal α-MnO_2 phase, as reported in the literature (Palaniyandy *et al.*, 2019). The presence of sharp and well-defined peaks indicates high crystallinity and phase purity, validating the effectiveness of the solvent-free mechanochemical synthesis approach.

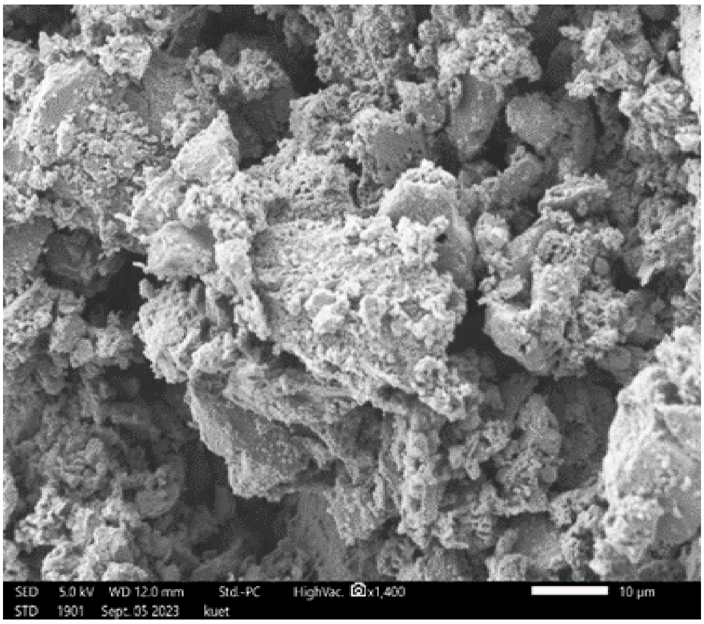

Figure 4. SEM images of the prepared MnO_2 material.

3.3 SEM Analysis

Scanning Electron Microscopy (SEM) was employed to examine the surface morphology of the synthesized MnO_2 material. The SEM micrograph, presented in **Figure 4**, reveals that the MnO_2 particles possess a distinctly porous structure. The material appears to be composed of agglomerated, irregularly shaped particles, each formed through the aggregation of smaller, uniformly sized grains. The presence of numerous pores on the surface is evident, suggesting a high surface area morphology. Such porosity is advantageous for electrochemical applications, as it can significantly enhance ion transport by providing more accessible active sites and reducing the diffusion path length for Zn^{2+} ions. These structural features are expected to contribute positively to the intercalation/deintercalation behavior during charge–discharge cycles, thereby improving the overall electrochemical performance of the MnO_2 cathode material.

3.4 EDS Analysis

Energy Dispersive X-ray Spectroscopy (EDS) was conducted to determine the elemental composition of the synthesized MnO_2 material. The corresponding EDS spectrum is presented in **Figure 5**. The analysis confirms that manganese (Mn) and oxygen (O) are the predominant elements present in the sample, with a relative mass percentage of approximately 68.07% for Mn and 31.93% for O. The absence of any extraneous elemental peaks indicates high purity of the prepared material, with no significant contamination from the synthesis process. These results validate the successful formation of MnO_2 as the principal phase in the synthesized nanoparticles, consistent with the expected stoichiometry and the findings from the XRD analysis.

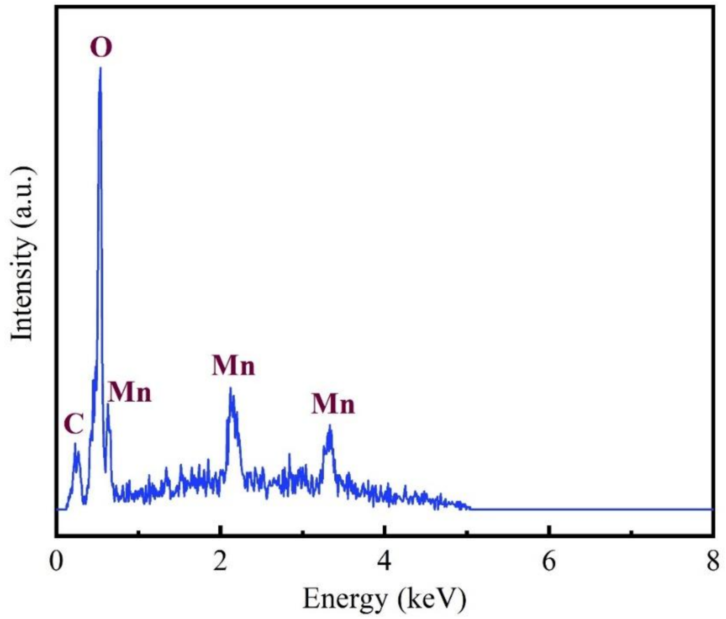

Figure 5: EDS spectrum of the prepared MnO_2 materials.

3.5 Cyclic Voltammetry (CV) of CR2032 Coin Cell Using MnO_2 as Cathode Material

Electrochemical characterization, particularly cyclic voltammetry (CV), plays a vital role in understanding the redox behavior, reversibility, and reaction mechanisms of electrode materials. **Figure 6** presents the CV curve of the CR2032 coin cell assembled using the synthesized MnO_2 as the cathode material. The CV measurements were carried out within a potential window of 0.8–1.9 V at a scan rate of 1 mV/s. The voltammogram reveals one prominent oxidation peak at approximately 1.58 V and two well-defined reduction peaks at around 1.31 V and 1.18 V, indicating reversible electrochemical processes (Corpuz *et al.*, 2020; Wang *et al.*, 2019). The oxidation peak near 1.58 V is attributed to the oxidation of metallic zinc (Zn) to Zn^{2+} at the anode, accompanied by the deintercalation of Zn^{2+} ions into the tunnel structure of MnO_2 at the cathode. This process corresponds to the partial transformation of MnO_2 into $ZnMnO_2$. During the reverse scan, the reduction peaks at 1.31 V and 1.18 V signify the de-intercalation of Zn^{2+} from the $ZnMnO_2$ structure, allowing MnO_2 to return to its original tunnel configuration. The presence of distinct and well-separated redox peaks highlights the electrochemical reversibility and stability of the MnO_2 cathode material, underscoring its potential suitability for use in aqueous rechargeable zinc-ion batteries.

Deintercalation reaction: $Zn = Zn^{2+} + 2e^-$

Intercalation reaction: $MnO_2 + Zn^{2+} + 2e^- = ZnMnO_2$
Overall cell reaction: $Zn + MnO_2 = ZnMnO_2$

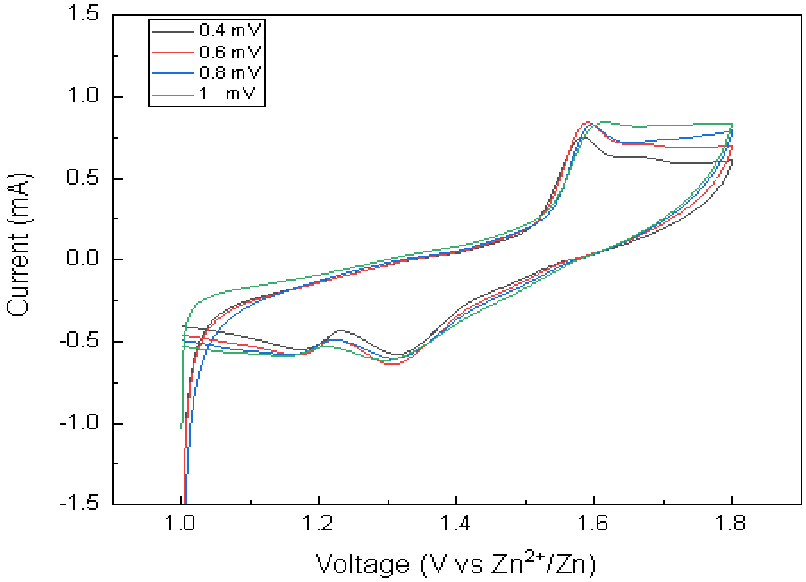

Figure 6: CV spectrum of CR2032 coin cell using MnO_2 as cathode materials.

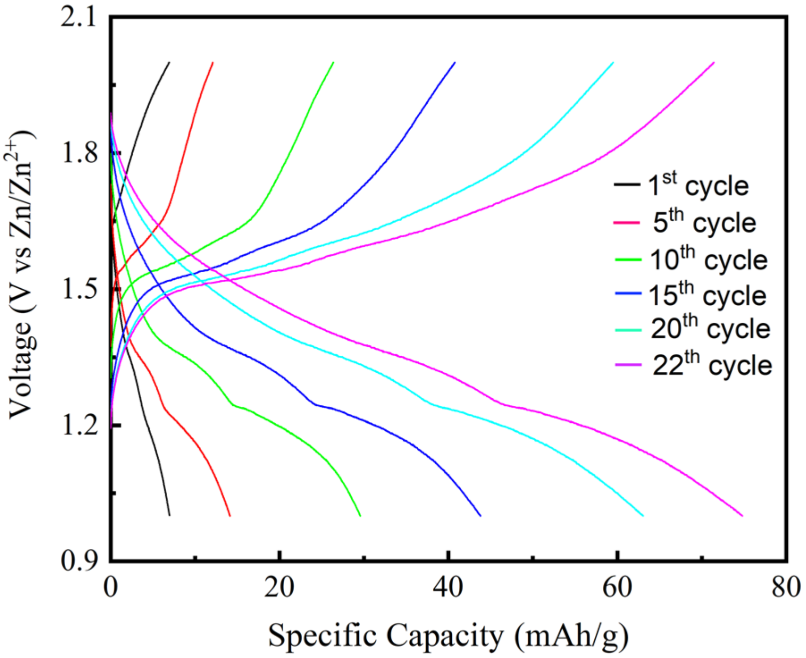

Figure 7: Cycling performance of CR2032 coin cell using MnO_2 material.

3.6 Battery Charge–Discharge (BCD) Performance

In order to assess the energy storage performance of the fabricated CR2032 coin cell, galvanostatic charge–discharge (GCD) measurements were conducted at a current density of 3 mA/g. The resulting charge–discharge profiles over multiple cycles, recorded at room temperature, are presented in Figure 7. The charge–discharge curves exhibit two distinct voltage plateaus, which closely correspond to the redox features observed in the cyclic voltammetry (CV) analysis. These plateaus are indicative of the two-step Zn^{2+} ion intercalation and deintercalation processes in the MnO_2 cathode structure. As the charge–discharge process progresses, a slight decrease in the plateau voltage is observed, which may be attributed to polarization effects and gradual structural rearrangements during cycling. The electrochemical reversibility of Zn^{2+} ion insertion/extraction into/from the MnO_2 host lattice is evidenced by the stable and repeatable plateaus over successive cycles. The coin cell was subjected to 22 charge–discharge cycles, achieving a high discharge capacity of 76 mAh/g and a charge capacity of 77 mAh/g by the 22nd cycle. Interestingly, the specific capacity showed a slight increase with cycling, which may be attributed to the progressive activation or phase transformation of the MnO_2 material within the electrode matrix. These results affirm the promising electrochemical performance and cycling stability of the MnO_2 cathode synthesized via the solvent-free mechanochemical approach, highlighting its potential for use in aqueous rechargeable zinc-ion battery systems.

4. CONCLUSIONS

In this study, MnO_2 was successfully synthesized using a solvent-free mechanochemical method and evaluated as a cathode material for aqueous rechargeable zinc-ion batteries (ARZIBs). The CR2032 coin cell assembled with the prepared MnO_2 cathode demonstrated stable electrochemical behavior and improved cycling performance over successive charge–discharge cycles, indicating good reversibility of Zn^{2+} intercalation/deintercalation. The findings highlight the potential of the solvent-free mechanochemical approach as a simple, cost-effective, and environmentally friendly method for fabricating MnO_2-based cathodes. Nevertheless, further optimization is required to enhance the electrochemical performance and achieve higher energy densities suitable for practical ARZIB applications.

ACKNOWLEDGEMENTS

The authors gratefully acknowledge the financial support provided by the University Grants Commission (UGC) of Bangladesh for conducting this research.

REFERENCES

Ahamed, P., Mollah, M. I. H., Hossain, M. S., Mim, R. S., Kundu, R., Ira, N. M., ... & Yousuf, M. A. (2023). Performances of MnO_2 and SnO_2 Coated MnO_2 as Cathode Materials for Aqueous Rechargeable Zinc-ion Batteries. *Journal of Science and Technology Research*, 5(1), 83-92.

Arshad, F., Li, L., Amin, K., Fan, E., Manurkar, N., Ahmad, A., ... & Chen, R. (2020). A comprehensive review of the advancement in recycling the anode and electrolyte from spent lithium ion batteries. *ACS Sustainable Chemistry & Engineering*, *8*(36), 13527-13554.

Blanc, L. E., Kundu, D., & Nazar, L. F. (2020). Scientific challenges for the implementation of Zn-ion batteries. *Joule*, *4*(4), 771-799.

Chamoun, M., Brant, W. R., Tai, C. W., Karlsson, G., & Noréus, D. (2018). Rechargeability of aqueous sulfate Zn/MnO_2 batteries enhanced by accessible Mn2+ ions. *Energy Storage Materials*, *15*, 351-360.

Chauhan, A., & Saini, R. P. (2014). A review on Integrated Renewable Energy System based power generation for stand-alone applications: Configurations, storage options, sizing methodologies and control. *Renewable and Sustainable Energy Reviews*, *38*, 99-120.

Corpuz, R. D., De Juan-Corpuz, L. M., Nguyen, M. T., Yonezawa, T., Wu, H. L., Somwangthanaroj, A., & Kheawhom, S. (2020). Binder-free α-MnO_2 nanowires on carbon cloth as cathode material for zinc-ion batteries. *International Journal of Molecular Sciences*, *21*(9), 3113.

Dehghani-Sanij, A. R., Tharumalingam, E., Dusseault, M. B., & Fraser, R. (2019). Study of energy storage systems and environmental challenges of batteries. *Renewable and Sustainable Energy Reviews*, 104, 192-208.

Deng, S., Wang, H., Liu, H., Liu, J., & Yan, H. (2014). Research progress in improving the rate performance of $LiFePO_4$ cathode materials. *Nano-Micro Letters*, *6*, 209-226.

Goodenough, J. B., & Kim, Y. (2010). Challenges for rechargeable Li batteries. *Chemistry of Materials*, *22*(3), 587-603.

Guan, S., Li, W., Ma, J., Lei, Y., Zhu, Y., Huang, Q., & Dou, X. (2018). A review of the preparation and applications of MnO_2 composites in formaldehyde oxidation. *Journal of Industrial and Engineering* Chemistry, 66, 126-140.

Hashemzadeh, F., Mehdi Kashani Motlagh, M., & Maghsoudipour, A. (2009). A comparative study of hydrothermal and sol–gel methods in the synthesis of MnO_2 nanostructures. *Journal of Sol-Gel Science and Technology*, *51*, 169-174.

Hilder, M., Winther-Jensen, B., & Clark, N. B. (2012). The effect of binder and electrolyte on the performance of thin zinc-air battery. *Electrochimica Acta*, *69*, 308-314.

Hu, P., Zhu, T., Wang, X., Zhou, X., Wei, X., Yao, X., ... & Mai, L. (2019). Aqueous Zn//Zn (CF_3SO_3) 2//Na_3V_2 (PO_4) 3 batteries with simultaneous Zn^{2+}/Na^{+} intercalation/de-intercalation. *Nano Energy*, *58*, 492-498.

Huang, J., Guo, Z., Ma, Y., Bin, D., Wang, Y., & Xia, Y. (2019). Recent progress of rechargeable batteries using mild aqueous electrolytes. *Small Methods*, 3(1), 1800272.

Huang, A., Zhou, W., Wang, A., Chen, M., Tian, Q., & Chen, J. (2021). Molten salt synthesis of α-MnO_2/Mn_2O_3 nanocomposite as a high-performance cathode material for aqueous zinc-ion batteries. *Journal of Energy Chemistry*, 54, 475-481.

Hu, Y., Zhu, H., Wang, J., & Chen, Z. (2011). Synthesis of layered birnessite-type manganese oxide thin films on plastic substrates by chemical bath deposition for flexible transparent supercapacitors. *Journal of Alloys and Compounds*, *509*(42), 10234-10240.

Idota, Y., Kubota, T., Matsufuji, A., Maekawa, Y., & Miyasaka, T. (1997). Tin-based amorphous oxide: a high-capacity lithium-ion-storage material. Science, 276(5317), 1395-1397.

Jiao, F., & Bruce, P. G. (2007). Mesoporous crystalline β-MnO_2 a reversible positive electrode for rechargeable lithium batteries. *Advanced Materials*, *19*(5), 657-660.

Liao, M., Wang, J., Ye, L., Sun, H., Wen, Y., Wang, C., & Peng, H. (2020). A deep-cycle aqueous zinc-ion battery containing an oxygen-deficient vanadium oxide cathode. *Angewandte Chemie*, *132*(6), 2293-2298.

Li, R., Zhang, H., Zheng, Q., & Li, X. (2020). Porous V_2O_5 yolk–shell microspheres for zinc ion battery cathodes: activation responsible for enhanced capacity and rate performance. *Journal of Materials Chemistry A*, *8*(10), 5186-5193.

Li, J. (2021). *Vanadium oxides and their derivatives as superb cathodes for aqueous zinc ion batteries* (Doctoral dissertation, UCL (Univerisity College London).

Lu, K., Song, B., Zhang, Y., Ma, H., & Zhang, J. (2017). Encapsulation of zinc hexacyanoferrate nanocubes with manganese oxide nanosheets for high-performance rechargeable zinc ion batteries. *Journal of Materials Chemistry A*, *5*(45), 23628-23633.

Ma, L., Chen, S., Long, C., Li, X., Zhao, Y., Liu, Z., & Zhi, C. (2019). Achieving high-voltage and high-capacity aqueous rechargeable zinc ion battery by incorporating two-species redox reaction. *Advanced Energy Materials*, *9*(45), 1902446.

Marepalli, P., Mathur, S. R., & Murthy, J. Y. (2020). Automatic differentiation approach for property computations in nanoscale thermal transport. *Computer Physics Communications*, *252*, 107138.

Meng, J., Song, Y., Qin, Z., Wang, Z., Mu, X., Wang, J., & Liu, X. X. (2022). Cobalt–Nickel Double Hydroxide toward Mild Aqueous Zinc-Ion Batteries. *Advanced Functional Materials*, *32*(33), 2204026.

Mim, R. S., Mollah, M. I. H., Kundu, R., Tonu, N. T., Hasan, M. M., Hossain, M. S., & Ahamed, P. (2023). Manganese Oxide Based Core@ Shell Nanoparticles and Its Application in Aqueous Zinc-Ion Battery. *Journal of Engineering Science*, 14(2), 69-77.

Nie, P., Shen, L., Luo, H., Ding, B., Xu, G., Wang, J., & Zhang, X. (2014). Prussian blue analogues: a new class of anode materials for lithium ion batteries. *Journal of Materials Chemistry A*, *2*(16), 5852-5857.

Palaniyandy, N., Kebede, M. A., Raju, K., Ozoemena, K. I., Le Roux, L., Mathe, M. K., & Jayaprakasam, R. (2019). α-MnO_2 nanorod/onion-like carbon composite cathode material for aqueous zinc-ion battery. *Materials Chemistry and Physics*, *230*, 258-266.

Parida, K. M., & Dash, S. S. (2009). Manganese containing MCM-41: Synthesis, characterization and catalytic activity in the oxidation of ethylbenzene. *Journal of Molecular Catalysis A: Chemical*, *306*(1-2), 54-61.

Serra, J. P., Fernandes, L. C., Pereira, N., Fidalgo-Marijuan, A., Porro, J. M., Costa, C. M., & Lanceros-Mendez, S. (2022). Humidity sensors based on magnetic ionic liquids blended in poly (vinylidene fluoride-co-hexafluoropropylene). *ACS Applied Polymer Materials*, *5*(1), 109-119.

Tang, N., Tian, X., Yang, C., Pi, Z., & Han, Q. (2010). Facile synthesis of α-MnO_2 nanorods for high-performance alkaline batteries. *Journal of Physics and Chemistry of Solids*, *71*(3), 258-262.

Tian, M., Liu, C., Zheng, J., Jia, X., Jahrman, E. P., Seidler, G. T., & Cao, G. (2020). Structural engineering of hydrated vanadium oxide cathode by K^{+} incorporation for high-capacity and long-cycling aqueous zinc ion batteries. *Energy Storage Materials*, *29*, 9-16.

Tonu, N. T., Yousuf, M. A., Ahamed, P., & Hasan, M. M. (2025). Development of bixbyite microdice fabricated cathode for aqueous rechargeable zinc ion batteries. *RSC Advances*, 15(19), 15318-15336.

Tonu, N. T., Ahamed, P., & Yousuf, M. A. (2024). Rice powder template for hausmannite Mn_3O_4 nanoparticles and its application to aqueous zinc ion battery. *Plos One*, 19(6), e0305611.

Tonu, N. T., Ahamed, P., & Yousuf, M. A. (2024). Bloom gelatin template based Mn_3O_4 nanoparticles synthesis for electrochemical application in aqueous rechargeable zinc ion battery. *Ionics*, 30(8), 4689-4703.

Wang, H., Lu, Z., Qian, D., Li, Y., & Zhang, W. (2007). Single-crystal α-MnO_2 nanorods: synthesis and electrochemical properties. *Nanotechnology*, *18*(11), 115616.

Wang, H. E., & Qian, D. (2008). Synthesis and electrochemical properties of α-MnO_2 microspheres. *Materials Chemistry and Physics*, *109*(2-3), 399-403.Xiang, Y., & Lu, S. (2012). Layer-by-layer self-assembly in the development of electrochemical energy conversion and storage devices from fuel cells to supercapacitors. *Chemical Society Reviews*, *41*(21), 7291-7321.

Wang, L., Wu, Q., Abraham, A., West, P. J., Housel, L. M., Singh, G., & Takeuchi, K. J. (2019). Silver-containing α-MnO_2 nanorods: electrochemistry in rechargeable aqueous Zn-MnO2 batteries. *Journal of the Electrochemical Society*, 166(15), A3575.

Xu, J., Thomas, H. R., Francis, R. W., Lum, K. R., Wang, J., & Liang, B. (2008). A review of processes and technologies for the recycling of lithium-ion secondary batteries. *Journal of Power Sources*, *177*(2), 512-527.

Xu, C., Li, B., Du, H., & Kang, F. (2012). Energetic zinc ion chemistry: the rechargeable zinc ion battery. *Angewandte Chemie International Edition*, *51*(4), 933-935.

Yang, J., Li, L., Yang, X., Song, S., Li, J., Jing, F., & Chu, W. (2019). Enhanced catalytic performances of in situ-assembled $LaMnO_3$/δ-MnO_2 hetero-structures for toluene combustion. *Catalysis Today*, *327*, 19-27.

Zhang, L., Chen, L., Zhou, X., & Liu, Z. (2015). Morphology-dependent electrochemical performance of zinc hexacyanoferrate cathode for zinc-ion battery. *Scientific Reports*, 5(1), 18263.

Zhang, T., Guo, Y., Li, C., Li, Y., Li, J., Zhao, F., & Ma, H. (2020). The effect of $LaFeO_3$@ MnO_2 on the thermal behavior of energetic compounds: An efficient catalyst with core-shell structure. *Advanced Powder Technology*, *31*(11), 4510-4516.

Zhang, Y., Liu, Y., Liu, Z., Wu, X., Wen, Y., Chen, H., ... & Peng, S. (2022). MnO_2 cathode materials with the improved stability via nitrogen doping for aqueous zinc-ion batteries. *Journal of Energy Chemistry*, *64*, 23-32.

Zhou, Y., Chen, F., Arandiyan, H., Guan, P., Liu, Y., Wang, Y., ... & Chu, D. (2021). Oxide-based cathode materials for rechargeable zinc ion batteries: Progresses and challenges. *Journal of Energy Chemistry*, *57*, 516-542.

© 2025 JES. *Journal of Engineering Science published by the Faculty of Civil Engineering, Khulna University of Engineering & Technology*. This is an open access article under the terms of the Creative Commons Attribution-Noncommercial-No Derivatives License, which permits use and distribution in any medium, provided the original work is properly cited, the use is non-commercial and no Modifications or adaptations are made.